Über die Aufspaltung einer Einzelblase beim Kollaps in der Nähe einer Wand

On the splitting of a single cavitation bubble during the collapse close to a wall

Max Koch[1], Christiane Lechner[1,2], Robert Mettin[1], Werner Lauterborn[1]

[1] *Univ. Göttingen, Drittes Physikalisches Institut, 37077 Göttingen, Email: max.koch@phys.uni-goettingen.de*

[2] *TU Wien, Institute of Fluid Mechanics & Heat Transfer*

Introduction

Since quite some decades the collapse of a cavitation bubble in front of a solid boundary is object of investigation. The physics behind this issue covers the fields of complex fluid dynamics, plasma physics, nonlinear acoustics, as well as non-equilibrium, two-phase thermodynamics. The history of modelling bubble dynamics started with reduced analytical models for spherical bubbles almost exactly a hundred years ago. When computational power increased, the boundary element method was introduced to study bubbles near boundaries, but mostly with incompressible formulations. Nowadays, advanced computational methods are able to resolve details on microsecond and even nanosecond time scales. One example of the relatively complex dynamical processes is the splitting of the collapsing bubble into several torus bubble rings, that has been observed in experiments many times, e.g. shown in Figure 1. From the finite volume simulations with a specialized two-phase solver we deduce that three phenomena are responsible for this splitting, that we call the "Blake splash", the "nanojet" and "microjet feed".

Physical model and numerical treatment

The authors have found a suitable way to numerically handle the nonlinear dynamics of a single cavitation bubble [1, 2, 3]. In this paper the authors present insight into the processes of bubble shape evolution when the liquid microjet forms by involution of the bubble and impacts onto the opposite side. Numerous experiments have been conducted on this case. Figure 1 shows experimentally photographed bubble collapses in the vicinity of a solid boundary. Due to the constricted liquid flow from the solid boundary side, the inflow towards the collapsing bubble from the "top" side is faster and thus induces a jet through the bubble, the *microjet*. On the side of the solid boundary several, partly shape unstable bubble torus rings are seen after jet impact (Fig. 1, frame 5). In this paper a hypothesis of the origin of these torus rings is proposed. The reader is referred to the aforementioned publications [1, 2, 3] for a detailed description of the following model, equations and numerical implementation, which are shown here in brevity.

The bubble is modelled nonlinearly compressible in both liquid and gas. Mass diffusion and heat transfer between both fluids are neglected. This neglect is justified, since the major dynamics is dominated by inertia and compressibility. Phase change effects are known to play a minor role for gas bubbles and are neglected as well for now. Viscosity of the liquid and surface tension are included. Gravity can be neglected, due to the short time scales and small dimensions of the bubbles. The numerical formulation has got only one velocity field $\vec{U}$ and one pressure field p for both phases liquid (l) and gas (g). The densities of the respective phases are computed via the barotropic equations $\rho_l(p)$ and $\rho_g(p)$: The gas, air here, is compressible according to the ideal gas law of adiabatic compression

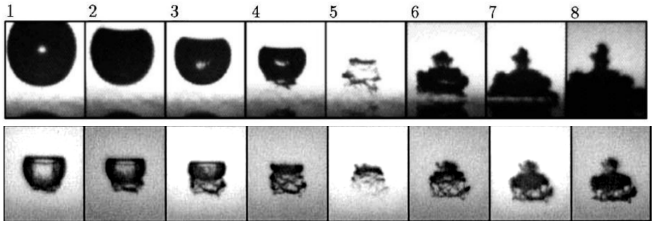

Figure 1: Bubble collapses close to a planar, solid boundary, as seen in experiments. Top: [4], interframe time is 17.7 µs; Bottom: [5], interframe time is 1 µs.

$$\mathcal{R}_{\text{spec}}\, T\, \rho_g = p, \tag{1}$$

$$p/\rho_g^{\kappa} = \text{const}, \tag{2}$$

with $\kappa = 1.4$ the ratio of specific heats for air and $\mathcal{R}_{\text{spec}}$ the specific gas constant, with value $287\,\text{J}/(\text{kg}\,\text{K})$. The liquid, water here, is compressible according to the Tait-Equation of state [6].

$$p(\rho_l) = (p_{l,n} + B)\left(\frac{\rho_l}{\rho_{l,n}}\right)^{\kappa_{\text{Tait}}} - B\,, \tag{3}$$

with $p_{l,n}$ the atmospheric pressure, $\rho_{l,n}$ the equilibrium density, B and κ_{Tait} the Tait parameters. The Tait Eq. (3) models isentropic fluids. Distinction between liquid and gas, is done by the *volume fraction* $\alpha_l \in [0, 1]$, where $\alpha_l = 0$ in the gas phase and $\alpha_l = 1$ in the liquid phase and in between on the interface. The overall density, for instance, is then written as

$$\rho(\vec{x}, t) = \alpha_l(\vec{x}, t)\rho_l(\vec{x}, t) + (1 - \alpha_l(\vec{x}, t))\,\rho_g(\vec{x}, t) \tag{4}$$

with ρ_l and ρ_g the densities of liquid and gas, respectively.

The Navier-Stokes equation, continuity equation and volume fraction advection equation – their formulation is omitted in this paper – are discretized using the finite volume and volume of fluid method incorporated

in the open source software package `foam-extend`, version 3.2, which is a branch-off from `OpenFOAM`. The solver the presented modifications base upon is called `compressibleInterFoam`. It contains a reformulation of the continuity equation in terms of the pressure p and solves all equations in a `PISO` loop (*pressure implicit with splitting of operators* [7]). The authors further implemented a mass preservation correction and the above equations of state, Eqs. (1) – (3).

Results

A single cavitation bubble is studied that expands from $R_{\text{start}} = 20\,\mu\text{m}$ at an initial distance to a solid boundary of $d_{\text{init}} = 639\,\mu\text{m}$ to the maximum radius of $R_{\text{max}} = 452\,\mu\text{m}$ and collapses again. In equilibrium, the radius would be $R_n = 164\,\mu\text{m}$, which defines the amount of gas inside. This gas amount is continuously reduced during expansion, in order to arrive at $R_n = 60\,\mu\text{m}$ for a stronger collapse. In the spherically symmetric case in an unbounded liquid, it would expand to $R_{\text{max,sph}} = 469\,\mu\text{m}$. It is common, to introduce a normalized distance to the solid boundary: $D^* = d_{\text{init}}/R_{\text{max,sph}}$ [8, 3]. In this sense, a "$D^* = 1.36$"-bubble is presented here and in [2]. In order to compute the case with high spatial resolution within reasonable time, the grid is set up in axial symmetry. The internal starting pressure of the bubble is determined by Eq. (1) and (2) and amounts to 85 292 bar. The liquid and gas are initially at rest, meaning $\vec{U} = 0$ everywhere, with an atmospheric pressure of 101315 Pa. The spatial resolution is homogeneous and highest in the bubble domain (cell width of 1 µm) and decreases smoothly towards the outer boundaries that were set to `waveTransmissive` and placed at a distance of $80\,R_{\text{max,sph}}$, except for the solid boundary.

Figure 2 shows the shockwave this bubble emits upon the first microsecond of expansion. The shockwave is reflected from the planar, solid boundary on the bottom of the frames and subsequently reflected as a tension wave at the bubble interface. The white line, indicating the bubble interface, is the isocontour line of $\alpha_l = 0.5$.

In the present paper, three different phenomena, responsible for torus bubble rings after collapse are described exemplarily.

Microjet feed, nanojet and Blake splash

Figure 3 sketches the three phenomena that are considered to be responsible for the splitting of the cavitation bubble during microjet impact. The bubble interface is drawn here in an axisymmetric manner, as indicated by the overlay drawing above the top row.

The first row of Fig. 3 sketches the geometrical event of simultaneous liquid flow from the microjet, bubble involution and bubble volume decrease. The high pressure zone of the impact, denoted here by the red dot, also travels upwards together with the intersection line of the microjet and bottom bubble interface. These effects together form the first phenomenon that is further denoted by the term *microjet feed*.

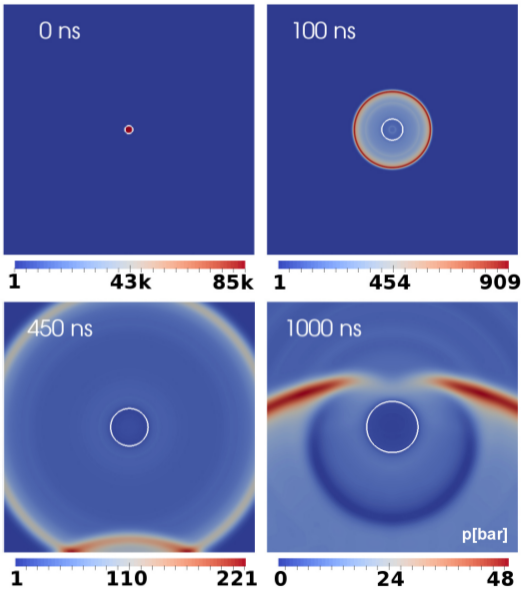

Figure 2: Shockwave emitted by the expanding bubble during the first microsecond and the reflection at the rigid wall and bubble interface. Taken from [2], bubble parameters: $D^* = d_{\text{init}}/R_{\text{max,sph}} = 1.36$, $R_{\text{max,sph}} = 469\,\mu\text{m}$.

The second row of Fig. 3 shows a smaller, yet nonetheless determinant phenomenon, the nanojet: At microjet impact, the gas inside the bubble is pressed with a velocity quite high in Mach number into the remainder of the bubble torus. On the liquid side of this gas jet lies the high pressure zone, as indicated with the red dot. As an effect, the annular liquid nanojet forms from the tip of the impact into the bubble. This phenomenon is only resolved at sufficiently high resolution. Here 450 cells per maximum bubble radius are needed, resulting in a cell width of 1 µm. At the tip of the nanojet (ring) droplets detach due to instabilities. When these droplets impinge onto the outer bubble interface, a small high pressure zone at the impinging spot is set up.

The bottom row of Fig. 3 shows a phenomenon which the authors denoted as the *Blake splash* [3]. The role of splashing effects in the dynamics of the splitting of the bubble has been studied for instance by Tong et al. [9] and Zhang et al. [10]. The authors describe how the microjet impact onto the opposite side of the bubble interface induces an annular indent on the outer interface that travels around the bubble like a surface wave. It is seen as a similar effect as the splash of a drop impact onto a flat free surface, but here onto a curved one. At microjet impact, a high pressure zone is formed, indicated by the red dot. When the bubble collapses close to the solid boundary, the injected liquid flow of the microjet hits the inflow of the liquid from the outside, forming the annular indent into the now torus shaped bubble.

The three phenomena described above have been observed in many of the calculations done by the authors and are considered stable phenomena driving the bubble shape deformation and splitting effects.

In the Figures 4 and 5 they are shown by way of example

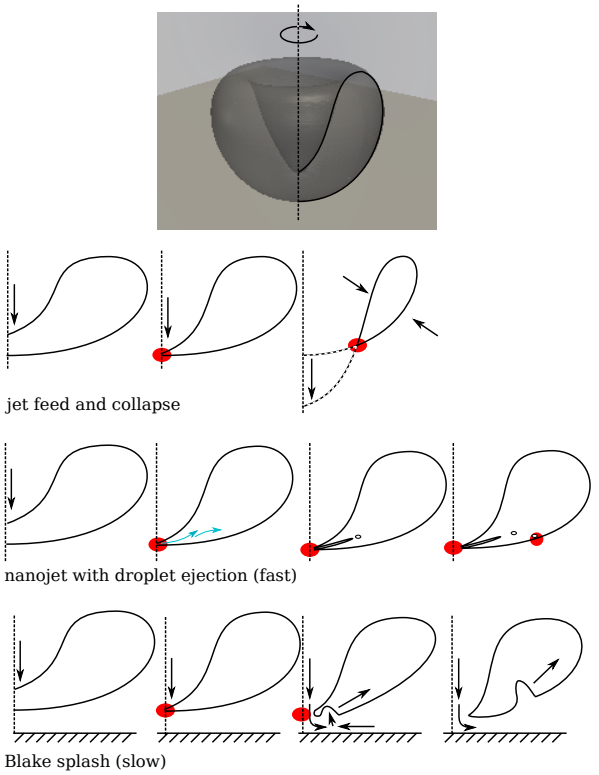

Figure 3: Sketch of the bubble splitting phenomena during microjet impact, as if they could be seperated.

by visualization of the pressure field of an axisymmetric calculation of the described "$D^* = 1.36$"-bubble, as published in [2]. In Fig. 4 the pressure field shortly after microjet impact is shown and the impact tip is again magnified for better visualization. The high pressure zone of the impact tip seems to drive the nanojet into the bubble remainder. Due to axis-symmetry reasons, the nanojet is of an annular ring shape. However, Hawker and Ventikos [11] claim that the nanojet keeps its annular shape even in a full 3D simulation, at least for some time.

Figure 5 shows the pressure field at two instances of time close to minimum bubble volume. At 94.10 µs the nanojet has already hit the outer bubble wall and two gas tori have been detached from the impact tip during microjet feed. 140 ns later, in the lower frame, three gas tori have been detached in total and the remainder bubble is pierced by the former nanojet. Very high pressures are emitted in rapid succession that generate complex shock and tension wave patterns at later times.

In order to demonstrate the Blake splash and the gas jet, the visualization of the velocity field of a simulation with different initial parameters, taken from [3], is shown in Fig. 6. The high Mach gas jet precedes the liquid nanojet and impinges onto the outer bubble interface in the left frame. It looks as if it would be reflected. The Blake splash lifts the outer bubble interface from below and thus turns and widens the base of the nanojet. Together with the ongoing microjet impact, in many cases this leads the nanojet to touch the inner bubble interface and therefore detach a gas torus.

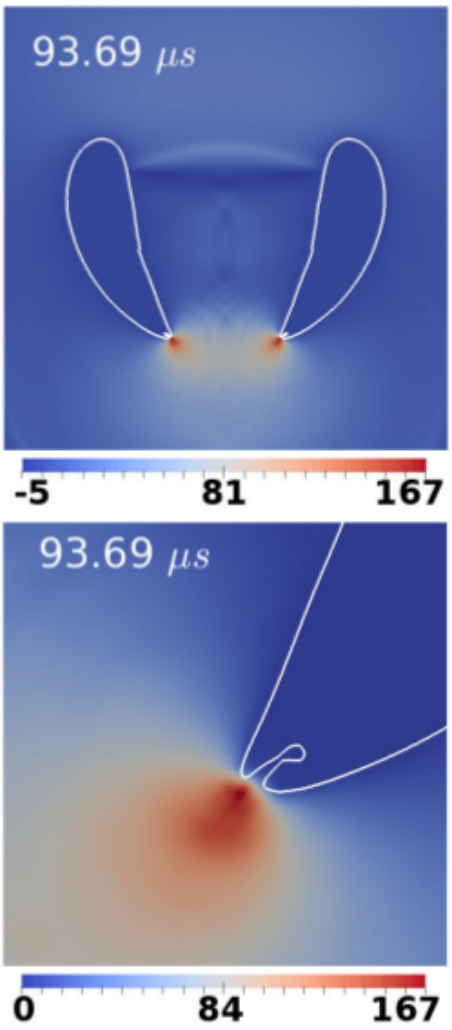

Figure 4: Torus bubble after microjet impact with the high pressure zone at impact tip. The onset of the nanojet is seen clearly in the magnification (bottom frame). Pressure field in bar. Taken from [2], bubble parameters: $D^* = d_{\mathrm{init}}/R_{\mathrm{max,sph}} = 1.36, R_{\mathrm{max,sph}} = 469\,\mu\mathrm{m}$.

Conclusion

Laser generated, single cavitation bubbles reveal a dynamics that includes the splitting of the bubble into several parts after liquid microjet impact. This has been seen many times in experiments and also in the simulations done here with a finite volume solver that fully includes nonlinear compressibility effects. The authors propose three separate phenomena that act together in the complex bubble splitting process: The *microjet feed*, the liquid annular *nanojet* and the *Blake splash*. The first phenomenon accounts for the geometrical issue of the continuously progressing intersection line of the microjet surface (involuted upper bubble interface) with the lower bubble interface and simultaneous overall bubble volume shrinking. The second phenomenon is an annular jet into the bubble stemming from the tip of the microjet impact zone. It was found by performing simulations with very high spatial resolution. The third has been proposed in literature as a similar effect as the splash of a drop impact onto a flat, free surface.

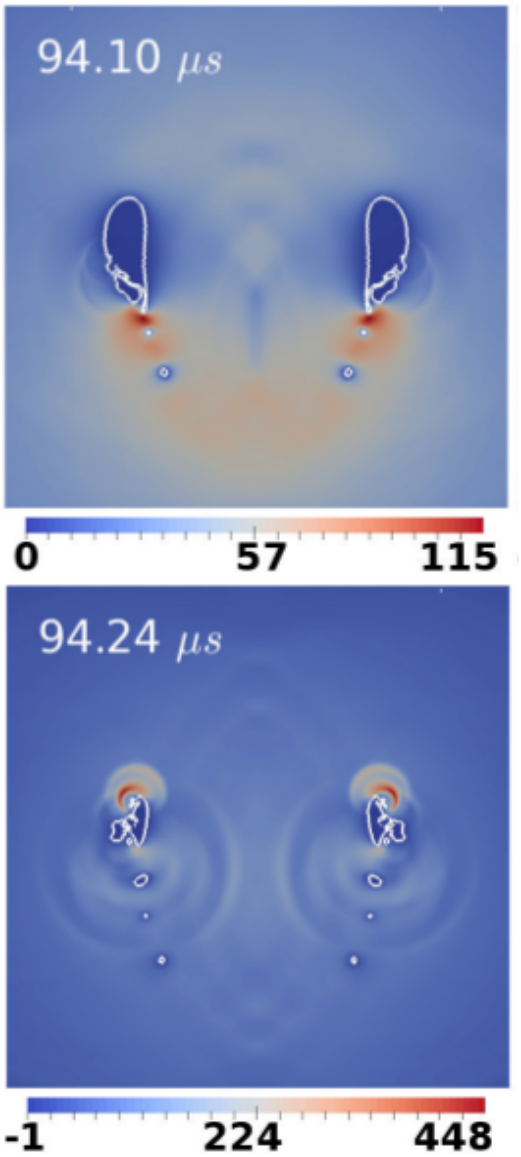

Figure 5: Bubble splitting with torus detachments (three gas rings – here an axisymmetric cut). Pressure in bar. Taken from [2], bubble parameters: $D^* = d_{\text{init}}/R_{\text{max,sph}} = 1.36$, $R_{\text{max,sph}} = 469\,\mu\text{m}$.

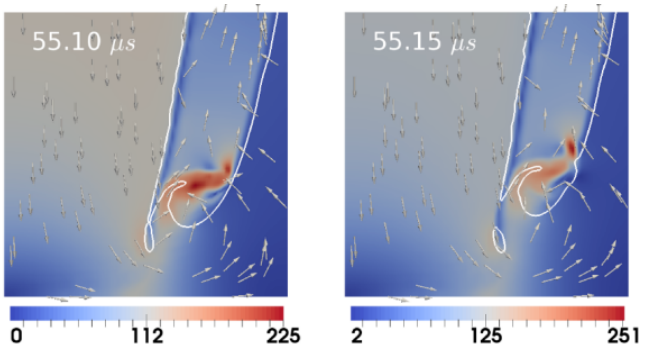

Figure 6: Velocity field in meter per second of a bubble collapse of different initial data than in Figures 2, 4 and 5. Clearly seen are the high Mach number gas jet and the nano-jet. The Blake splash lifts the outer bubble interface. Taken from [3], bubble parameters: $D^* = 1.02, R_{\text{max}} = R_{\text{start}} = 500\,\mu\text{m}$.

Acknowledgements

This work has been supported by the Deutsche Forschungsgesellschaft (German research foundation), project No. ME 1645/8-1.

References

[1] M. Koch, C. Lechner, F. Reuter, K. Köhler, R. Mettin, and W. Lauterborn. Numerical modeling of laser generated cavitation bubbles with the finite volume and volume of fluid method, using OpenFOAM. *Computers and Fluids*, 126:71–90, 2016.

[2] C. Lechner, M. Koch, W. Lauterborn, and R. Mettin. Pressure and tension waves from bubble collapse near a solid boundary: A numerical approach. *Journal of the Acoustical Society of America*, 142(6):3649–3659, 2017.

[3] W. Lauterborn, C. Lechner, M. Koch, and R. Mettin. Bubble models and real bubbles: Rayleigh and energy-deposit cases in a Tait-compressible liquid. *IMA Journal of Applied Mathematics*, 2018. accepted.

[4] C.-D. Ohl, A. Philipp, and W. Lauterborn. Cavitation bubble collapse studied at 20 million frames per second. *Annalen der Physik*, 4:26–34, 1995.

[5] A. Philipp and W. Lauterborn. Cavitation erosion by single laser-produced bubbles. *Journal of Fluid Mechanics*, 361:75–116, 1998.

[6] Yuan-Hui Li. Equations of state of water and sea water. *Journal of Geophysical Research*, 72(10):2665–2678, 1967.

[7] J. H. Ferziger and M. Perić. *Computational Methods for Fluid Dynamics*. Springer, 1997.

[8] M. S. Plesset and R. B. Chapman. Collapse of an initially spherical vapour cavity in the neighbourhood of a solid boundary. *Journal of Fluid Mechanics*, 47:283–290, 1971.

[9] R. R. Tong, W. P. Schiffers, S. J. Shaw, J. R. Blake, and D. C. Emmony. The role of 'splashing' in the collapse of a laser-generated cavity near a rigid boundary. *Journal of Fluid Mechanics*, 380:339–361, 1999.

[10] A. M. Zhang, S. Li, and J. Cui. Study on splitting of a toroidal bubble near a rigid boundary. *Physics of Fluids*, 27(6):062102(1–16), 2015.

[11] N. A. Hawker and Y. Ventikos. Interaction of a strong shockwave with a gas bubble in a liquid medium: a numerical study. *Journal of Fluid Mechanics*, 701:59–97, 2012.